

New upper limits on low-frequency radio emission from isolated neutron stars with LOFAR

I. Pastor-Marazuela^{1,2}, S. M. Straal³, J. van Leeuwen², and V. I. Kondratiev²

¹ Anton Pannekoek Institute for Astronomy, University of Amsterdam, Science Park 904, PO Box 94249, 1090 GE Amsterdam, The Netherlands

e-mail: ines.pastormarazuela@uva.nl

² ASTRON, the Netherlands Institute for Radio Astronomy, PO Box 2, 7790 AA Dwingeloo, The Netherlands

³ NYU Abu Dhabi, PO Box 129188, Abu Dhabi, United Arab Emirates

January 16, 2023

ABSTRACT

Neutron stars that show X-ray and γ -ray pulsed emission must, somewhere in the magnetosphere, generate electron-positron pairs. Such pairs are also required for radio emission, but then why do a number of these sources appear radio quiet? Here, we carried out a deep radio search towards four such neutron stars that are isolated X-ray/ γ -ray pulsars but for which no radio pulsations have been detected yet. These sources are 1RXS J141256.0+792204 (Calvera), PSR J1958+2846, PSR J1932+1916 and SGR J1907+0919. Searching at lower radio frequencies, where the radio beam is thought to be wider, increases the chances of detecting these sources, compared to the earlier higher-frequency searches. We thus carried a search for periodic and single-pulse radio emission with the LOFAR radio telescope at 150 MHz. We used the known periods, and searched a wide range of dispersion measures, as the distances are not well constrained. We did not detect pulsed emission from any of the four sources. However, we put very constraining upper limits on the radio flux density at 150 MHz, of $\lesssim 1.4$ mJy.

Key words. Stars: neutron – pulsars: general

1. Introduction

Through their spin and magnetic field, neutron stars act as powerful cosmic dynamos that can generate a wide variety of electromagnetic emission. There thus exist many subclasses of neutron stars, with different observed behavior. The evolutionary links between some of the classes are established, while for others these connections are currently unknown. The largest group in this varied population is formed by the regular rotation-powered radio pulsars. The fast spinning, high magnetic field influx to this group are the young pulsars. These show a high spin-down energy loss rate \dot{E} , and a number of energetic phenomena such as radio giant pulse (GP) emission. The most extreme of these fast-spinning and/or high-field sources could potentially also power Fast Radio Bursts (FRBs; e.g. Pastor-Marazuela et al. 2022). On the long-period outskirts of the P - \dot{P} diagram, slowly-rotating pulsars (e.g. Young et al. 1999; Tan et al. 2018) and magnetars (e.g. Caleb et al. 2022; Hurley-Walker et al. 2022) sometimes continue to shine.

Some neutron stars, however, only shine intermittently at radio frequencies. The rotating radio transients (RRATs) burst very irregularly, and in the P - \dot{P} diagram most are found near the death line (Keane et al. 2011), between the canonical radio pulsars and magnetars. The exact evolutionary connection between RRATs and the steadily radiating normal pulsars is unclear, but studies suggest the presence of an evolutionary link between these different classes (e.g. Burke-Spolaor 2012).

Finally, populations of neutron stars exist that appear to not emit in radio at all: radio-quiet magnetars such as most anomalous X-ray pulsars (AXPs) and soft gamma repeaters (SGRs), X-ray dim isolated neutron stars (XDINSs; Haberl 2007), and

γ -ray pulsars (e.g. Abdo et al. 2013). These are able to produce high-energy emission but are often radio quiet. (Gençali & Er-tan 2018) proposed RRATs can evolve into XDINSs through a fallback accretion disk, thus becoming radio quiet. However, the magnetar SGR 1935+2154 was recently seen to emit a bright radio burst bridging the gap in radio luminosities between regular pulsars and FRBs (CHIME/FRB Collaboration 2020; Bochenek et al. 2020; Maan et al. 2022b). This suggests magnetars could explain the origin of some, if not all, extragalactic FRBs.

Potentially, some of these could produce radio emission only visible at low radio frequencies. Detections of radio pulsations of the γ and X-ray pulsar *Geminga*, PSR J0633+1746, have been claimed at and below the 100 MHz observing frequency range (Malofeev & Malov 1997; Malov et al. 2015; Maan 2015), although a very deep search using the low frequency array (LOFAR van Haarlem et al. 2013) came up empty (Ch. 6 in Coenen 2013). Such low-frequency detections offer an intriguing possibility to better understand the radio emission mechanism of these enigmatic objects. Radio detections of a magnetar with LOFAR, complementary to higher-frequency studies such as Camilo et al. (2006) and Maan et al. (2022a) for XTE J1810–197, could offer insight into emission mechanisms and propagation in ultra-strong magnetic fields.

XDINSs feature periods that are as long as those in magnetars, but they display less extreme magnetic field strength. The XDINSs form a small group of seven isolated neutron stars that show thermal emission in the soft X-ray band. Since their discovery with ROSAT in the 1990s, several attempts were made to detect these sources at radio frequencies, but they were unsuccessful (e.g. Kondratiev et al. 2009). As those campaigns operated above 800 MHz, a sensitive lower-frequency search

arXiv:2301.05509v1 [astro-ph.HE] 13 Jan 2023

could be opportune. It has been proposed (e.g. Komesaroff 1970; Cordes 1978) and observed (e.g. Chen & Wang 2014) that pulsar profiles are usually narrower at higher frequencies and become broader at lower radio frequencies. This suggests the radio emission cone is broader at low frequencies, and sweeps across a larger fraction of the sky as seen from the pulsar. Additionally, radio pulsars often present negative spectral indices, and are thus brighter at lower frequencies (Bilous et al. 2016). If all neutron star radio beams are broader and brighter at lower frequencies, chances of detecting radio emission from γ and X-ray Isolated Neutron Stars (INSs) increase at the lower radio frequencies offered through LOFAR. The earlier observations that resulted in non-detections could then have just missed the narrower high-frequency beam, where the wider lower-frequency beam may, in contrast, actually enclose Earth. In that situation, LOFAR could potentially detect the source.

Recently, a number of radio pulsars were discovered that shared properties with XDINSs and RRATs, such as soft X-ray thermal emission, a similar position in the P - \dot{P} diagram, and a short distance to the solar system. These sources, PSR J0726–2612 (Rigoselli et al. 2019) and PSR J2251–3711 (Morello et al. 2020), support the hypothesis that XDINSs are indeed not intrinsically radio quiet, but have a radio beam pointed away from us. These shared properties could reflect a potential link between the radio and X-ray emitting pulsars with XDINSs and RRATs. A firm low-frequency radio detection of INSs would thus tie together these observationally distinct populations of neutron stars.

In this work we present LOFAR observations of four INSs that brightly pulsate at X-ray or γ -ray energies, but have not been detected in radio. These sources are listed in Section 2, and their parameters are presented in Table 1.

2. Targeted sources

2.1. J1412+7922

The INS 1RXS J141256.0+792204, dubbed "Calvera" and hereafter J1412+7922, was first detected with *ROSAT* (Voges et al. 1999) as an X-ray point source, and subsequently with *Swift* and *Chandra* (Rutledge et al. 2008; Shevchuk et al. 2009). X-ray observations confirmed its neutron star nature through the detection of $P \simeq 59$ ms pulsations by Zane et al. (2011), and allowed for the determination of its spin-down luminosity $\dot{E} \sim 6 \times 10^{35}$ erg s⁻¹, characteristic age $\tau_c \equiv P/2\dot{P} \sim 3 \times 10^5$ years, and surface dipole magnetic field strength $B_s = 4.4 \times 10^{11}$ G by Halpern et al. (2013). Although these values are not unusual for a rotationally-powered pulsar, the source is not detected in radio (Hessels et al. 2007; Zane et al. 2011) or γ -rays (Mereghetti et al. 2021). The X-ray emission can be modelled with a two-temperature black body spectrum (Zane et al. 2011), similar to other XDINS (Pires et al. 2014). However, J1412+7922 shows a spin period much faster than typically observed in XDINS. Since the source is located at high galactic latitudes and its inferred distance is relatively low (~ 3.3 kpc; Mereghetti et al. 2021) the path through the interstellar medium is not long enough to explain the radio non-detections by high dispersion measure (DM) or scattering values.

2.2. J1958+2846

Discovered by Abdo et al. (2009) through a blind frequency search of *Fermi-LAT* γ -ray data, INS PSR J1958+2846, hereafter J1958+2846, has shown no X-ray or radio continuum emis-

sion counterpart so far (Ray et al. 2011; Frail et al. 2016). Arecibo observations have put very constraining upper limits of 0.005 mJy at 1510 MHz (Ray et al. 2011). Searches for pulsations from the source using the single international LOFAR station FR606 by Grießmeier et al. (2021) also found no periodic signal.

The double-peaked pulse profile of J1958+2846 can be interpreted as a broad γ -ray beam. The earlier higher-frequency radio non-detections could be due to a narrower radio beam and to an unfavourable rotation geometry with respect to the line of sight. If the radio beam is indeed wider at lower frequencies, LOFAR would have higher chances of detecting it. In that case, a setup more sensitive than the Grießmeier et al. (2021) single-station search is required.

Modeling by Pierbattista et al. (2015) indicates that the γ -ray pulse profile of J1958+2846 can be well fitted by One Pole Caustic emission (OPC, Romani & Watters 2010, Watters et al. 2009) or an Outer Gap model (OG, Cheng et al. 2000). In both cases, the γ -rays are generated at high altitudes above the NS surface. Each model constrains the geometry of the pulsar. For the OPC model, the angle between the rotation and magnetic axes $\alpha = 49^\circ$, while the angle between the observer line-of-sight and the rotational axis $\zeta = 85^\circ$. The OG model reports similarly large angles, with the NS equator rotating in the plane that also contains Earth, and an oblique dipole: $\alpha = 64^\circ$, $\zeta = 90^\circ$. If this model is correct, the low-frequency radio beam would thus need to be wider than $\sim 30^\circ$ to encompass the telescope. That is uncommonly wide; only 8 out of the 600 pulsars in the ATNF catalogue that are not recycled and have a published 400 MHz flux, have a duty cycle suggestive of a beam wider than 30% (Manchester et al. 2005). As such a width is unlikely, a total-intensity detection would thus suggest to first order a geometry where α and ζ are closer than follows from Pierbattista et al. (2015), even if that suggestion would only be qualitative. Subsequent follow-up measurements of polarisation properties throughout the pulse, and fitting these to the rotating vector model (RVM; Radhakrishnan & Cooke 1969), can quantify allowed geometries to within a relatively precise combinations of α and ζ . As a matter of fact, in a similar study on radio-loud γ -ray pulsars, Rookyard et al. (2015) already find that RVM fits suggest that the magnetic inclination angles α are much lower than predicted by the γ -ray light curve models. This, in turn, affirms that deep radio searches can lead to detections even when the γ -ray light curves suggest the geometry is unfavorable.

2.3. J1932+1916

The INS PSR J1932+1916, hereafter J1932+1916, was discovered in *Fermi-LAT* data through blind searches with the *Einstein@Home* volunteer computing system (Clark et al. 2017). J1932+1916 is the youngest and γ -ray brightest among the four γ -ray pulsars presented from that effort in (Pletsch et al. 2013). The period is 0.21 s, the characteristic age is 35 kyr. Frail et al. (2016) find no continuum 150 MHz source at this position with GMRT at a flux density upper limit of 27 mJy beam⁻¹, with 1σ errors. If the flux density they find at the position of the pulsar is in fact the pulsed emission from J1932+1916, then a LOFAR periodicity search as described here should detect the source at a S/N of 15 if the duty cycle is 10%. Karpova et al. (2017) report on a potential pulsar wind nebula (PWN) association from *Swift* and *Suzaku* observations. However, no X-ray periodicity searches have been carried out before.

2.4. J1907+0919

The Soft Gamma Repeater J1907+0919, also known as SGR 1900+14, was detected through its bursting nature by Mazets et al. (1979). Later outbursts were detected in 1992 (Kouveliotou et al. 1993), 1998 (Hurley et al. 1999) and 2006 (Mereghetti et al. 2006). The August 1998 outburst allowed the detection of an X-ray period of ~ 5.16 s, and thus confirmed the nature of the source as a magnetar (Hurley et al. 1999; Kouveliotou et al. 1999). Frail et al. (1999) detected a transient radio counterpart that appeared simultaneous to the 1998 outburst, and they identified the radio source as a synchrotron emitting nebula. Shitov et al. (2000) claimed to have found radio pulsations at 111 MHz from four to nine months after the 1998 burst, but the number of trials involved in the search, the small bandwidth of the system, and the low S/N of the presented plots, lead us to conclude the confidence level for these detections is low. No other periodic emission has been found at higher radio frequencies (Lorimer & Xilouris 2000; Fox et al. 2001; Lazarus et al. 2012).

This paper is organised as follows: in Section 3 we explain how we used LOFAR (van Haarlem et al. 2013) to observe the sources mentioned above; in Section 4 we detail the data reduction procedure, including the periodicity and the single pulse searches that we carried; in Section 5 we present our results, including the upper limit that we set on the pulsed emission; in Section 6 we discuss the consequences of these non-detections for the radio-quiet pulsar population, and in Section 7 we give our conclusions on this work.

3. Observations

We observed the four sources with the largest possible set of High Band Antennas (HBAs) that LOFAR can coherently beam form. Each observation thus added 22 HBA Core Stations, covering 78.125 MHz bandwidth in the 110 MHz to 190 MHz frequency range (centered on 148.92 MHz), with 400 channels of 195 kHz wide. The LOFAR beam-forming abilities allow us to simultaneously observe different regions of the sky (van Leeuwen & Stappers 2010; Stappers et al. 2011; Coenen et al. 2014). For our point-source searches of INs, we used three beams per observation; one beam pointed to the source of interest, one on a nearby known pulsar, and one as a calibrator blank-sky beam to cross-check potential candidates as possibly arising from Radio Frequency Interference (RFI). We carried out observations between 16 January 2015 and 15 February 2015 under project ID LC3_036¹. We integrated for 3 hours on each of our sources. The data was taken in Stokes I mode. Since the periods of the γ -ray pulsars are known, the time resolution of each observation was chosen such to provide good coverage of the pulse period, at a sampling time between 0.16–1.3 ms. The observation setup is detailed in Table 1.

4. Data reduction

The data was pre-processed by the LOFAR pulsar pipeline after each observation (Alexov et al. 2010; Stappers et al. 2011) and stored on the LOFAR Long Term Archive² in PSRFITS format

¹ After we completed the current manuscript as Pastor-Marazuela (2022, PhD Thesis, Ch. 2), Arias et al. (2022) posted a pre-print presenting partly the same data.

² LTA: <https://lta.lofar.eu/>

(Hotan et al. 2004). The 1.5 TB of data was then transferred to one of the nodes of the Apertif real-time FRB search cluster ARTS (van Leeuwen 2014; van Leeuwen et al. 2022).

We performed a periodicity search as well as a single-pulse search using PRESTO³ (Ransom 2001). The data was cleaned of RFI using first `rfi.find`, and then removing impulsive and periodic signals at $DM=0$ pc cm⁻³. Next we searched the clean data for periodic signals and single pulses. We searched for counterparts around the known P and \dot{P} of each pulsar. Additionally, we performed a full blind search in order to look for potential pulsars in the same field of view, since many new pulsars are found at low frequencies (Sanidas et al. 2019) and chance discoveries happen regularly (e.g., Oostrum et al. 2020). Since the DM of our sources is unknown, we searched over a range of DMs going from 4 pc cm⁻³ to 400 pc cm⁻³. The DM-distance relation is not precise enough to warrant a much smaller DM range, even for sources for which a distance estimate exists; and a wider DM range allows for discovery of other pulsars contained in our field of view. The highest DM pulsar detected with LOFAR has a $DM = 217$ pc cm⁻³ (Sanidas et al. 2019). We thus searched up to roughly twice this value to make sure that any detectable sources were covered. We determined the optimal de-dispersion parameters with `DDplan` from PRESTO. The sampling time variation between some of the four observations had a slight impact on the exact transitions of the step size but generally the data was de-dispersed in steps of 0.01 pc cm⁻³ up to $DM = 100$ pc cm⁻³; then by 0.03 pc cm⁻³ steps up to 300 pc cm⁻³ and finally using 0.05 pc cm⁻³ steps.

We manually inspected all candidates down to $\sigma = 4$, resulting in ~ 1400 candidates per beam. To verify our observational setup, we performed the same blind search technique to our test pulsars B1322+83 and B1933+16, which we detected. The test pulsar B1953+29 was not detected because the sampling time of the observation of J1958+2846 was not adapted to its ~ 6 ms period. However, we were able to detect B1952+29 (Hewish et al. 1968) in this same pointing. Even though it is located at $>1^\circ$ from the targeted coordinates, it is bright enough to be visible as a side-lobe detection.

The candidates from PRESTO's single pulse search were further classified using the deep learning classification algorithm developed by Connor & van Leeuwen (2018), which has been verified and successful in the Apertif surveys (e.g. Connor et al. 2020; Pastor-Marazuela et al. 2021). This reduced the number of candidates significantly by sifting out the remaining RFI. The remaining candidates were visually inspected.

5. Results

In our targeted observations we were unable to detect any plausible astronomical radio pulsations or single pulses. We determine new 150 MHz flux upper limits by computing the sensitivity limits of our observations. To establish these sensitivity limits, we apply the radiometer equation adapted to pulsars, detailed below. We determine the telescope parameters that are input to this equation by following the procedure⁴ described in Kondratiev et al. (2016) and Mikhailov & van Leeuwen (2016). That approach takes into account the system temperature (including the sky temperature), the projection effects governing the effective area of the fixed tiles, and the amount of time and bandwidth removed due to RFI, to produce

³ PRESTO: <https://www.cv.nrao.edu/~sransom/presto/>

⁴ https://github.com/vkond/LOFAR-BF-pulsar-scripts/blob/master/fluxcal/lofar_fluxcal.py

Table 1. Parameters of the observed pulsars and observational setup of the observations in the LC3_036 proposal. The beam of each observation was centered in the reported pulsar coordinates. Listed in the bottom rows are the earlier periodicity and single pulse search limits. The upper limits from [Frail et al. \(2016\)](#) described in the main text are period-averaged flux densities and are not listed here. The last row lists the limits from the current work, for $S/N=5$, with errors of 50% ([Bilous et al. 2016](#)).

	J1412+7922	J1958+2846	J1932+1916	J1907+0919
Right ascension, α (J2000)	14 12 56	19 58 40	19 32 20	19 07 14.33
Declination, δ (J2000)	+79 22 04	+28 45 54	+19 16 39	+09 19 20.1
Period, P (s)	0.05919907107	0.29038924475	0.208214903876	5.198346
Period derivative, \dot{P} (s s ⁻¹)	3.29134×10^{-15}	2.12038×10^{-13}	9.31735×10^{-14}	9.2×10^{-11}
Epoch (MJD)	58150 ^a	54800 ^b	55214 ^c	53628 ^d
LOFAR ObsID	L257877	L258545	L259173	L216886
Obs. date (MJD)	57038	57046	57068	56755
Sample time (ms)	0.16384	1.31072	1.31072	0.65536
Test pulsar detected	B1322+83	B1952+29	B1933+16	B1907+10
Periodic flux density (mJy @ GHz)	<4 @ 0.385 ^e <0.05 @ 1.36 ^f <0.3 @ 1.38 ^e	<2.0 @ 0.15 ^g <0.005 @ 1.51 ^b	<2.9 @ 0.15 ^g <0.075 @ 1.4 ^c	50 @ 0.111 ^h <0.4 @ 0.43 ⁱ <0.3 @ 1.41 ⁱ <0.012 @ 1.95 ^j
LOFAR periodic sensitivity $S_{\text{lim,p}}$ (mJy) ..	0.26 ± 0.13	0.53 ± 0.26	0.73 ± 0.36	1.39 ± 0.69
LOFAR single pulse sensitivity $S_{\text{lim,sp}}$ (Jy)	1.47 ± 0.73	1.35 ± 0.68	2.20 ± 1.10	0.84 ± 0.82

Notes. ^a[Bogdanov et al. \(2019\)](#), ^b[Ray et al. \(2011\)](#), ^c[Pletsch et al. \(2013\)](#), ^d[Mereghetti et al. \(2006\)](#), ^e[Hessels et al. \(2007\)](#), ^f[Zane et al. \(2011\)](#), ^g[Grießmeier et al. \(2021\)](#), ^h[Shitov et al. \(2000\)](#), ⁱ[Lorimer & Xilouris \(2000\)](#), ^j[Lazarus et al. \(2012\)](#)

the overall observation system-equivalent flux density (SEFD).

For the sensitivity limit on the periodic emission we use the following equation (see., e.g., [Dewey et al. 1985](#)):

$$S_{\text{lim,p}} = \beta \frac{T_{\text{sys}}}{G \sqrt{n_p} \Delta\nu t_{\text{obs}}} \times S/N_{\text{min}} \times \sqrt{\frac{W}{P - W}}, \quad (1)$$

where $\beta \lesssim 1$ is a digitisation factor, T_{sys} (K) is the system temperature, G (K Jy⁻¹) is the telescope gain, $\Delta\nu$ (Hz) is the observing bandwidth, and t_{obs} (s) is the observation time. P (s) represents the spin period, while W (s) gives the pulsed width assuming a pulsar duty cycle of 10%. To facilitate direct comparison of the periodic emission limits to values reported in e.g., [Ray et al. \(2011\)](#) and [Grießmeier et al. \(2021\)](#), we use a minimum signal-to-noise ratio $S/N_{\text{min}} = 5$. A more conservative option, given the high number of candidates per beam, would arguably be to use a limit of $S/N=8$. We did, however, review by eye all candidates with $S/N>4$; and the reader can easily scale the reported sensitivity limits to a different S/N value.

The sensitivity limit on the single pulse emission, $S_{\text{lim,sp}}$, is computed as follows:

$$S_{\text{lim,sp}} = \beta \frac{T_{\text{sys}}}{G \sqrt{n_p} \Delta\nu t_{\text{obs}}} \times S/N_{\text{min}} \times \sqrt{\frac{t_{\text{obs}}}{W}}, \quad (2)$$

where all variables are the same as in Equation 2. We searched for single pulses down to a signal-to-noise ratio $S/N_{\text{min}} = 7$.

We report these periodic and single pulse sensitivity limits, computed at the coordinates of the central beam of each observation, in Table 1. Even though all observations are equally long, the estimated $S_{\text{lim,p}}$ values are different. That is mostly due to the strong dependence of the LOFAR effective area, and hence the sensitivity, on the elevation.

In Fig. 1, we compare our upper limits to those established in previous searches, mostly using the same techniques. Our upper

limit on the flux of J1907+0919 is $\sim 50\times$ deeper than the claimed 1998-1999 detections, at the same 3-m wavelength, with BSA ([Shitov et al. 2000](#)). Other searches were generally undertaken at higher frequencies ([Hessels et al. 2007](#); [Zane et al. 2011](#); [Ray et al. 2011](#); [Pletsch et al. 2013](#); [Grießmeier et al. 2021](#)). If we assume that these four pulsars have radio spectra described by a single power-law $S_\nu \propto \nu^\alpha$ with a spectral index of $\alpha = -1.4$ ([Bates et al. 2013](#); [Bilous et al. 2016](#)), the upper limits we present here for J1412+7922 and J1932+1916 are the most stringent so far for any search. The upper limits on J1958+2846 ([Arecibo](#); [Ray et al. 2011](#)) and J1907+0919 ([GBT](#); [Lazarus et al. 2012](#)) are a factor of 2–3 more sensitive than ours. However, pulsars present a broad range of spectral indices. If we take the mean $\pm 2\sigma$ measured by [Jankowski et al. \(2018\)](#), spectral indices can vary from -2.7 to -0.5 . The flux upper limits we measure would be the deepest assuming a -2.7 spectral index, but the shallowest at -0.5 .

6. Discussion

6.1. Comparison to previous limits

For J1958+2846 and J1932+1916, we can make a straightforward relative comparisons between our results presented here and the existing limit at 150 MHz, from the single-station LOFAR campaign by [Grießmeier et al. \(2021\)](#). Our 22 Core Stations are each 1/4th of the area of the FR606 station and are coherently combined, leading to a factor $\frac{A_{\text{core}}}{A_{\text{FR606}}} = \frac{22}{4}$ difference in area A for the radiometer equation and S_{lim} . The integration time t of 3 h is shorter than the FR606 total of 8.3 h (J1958+2846) and 4.1 h (J1932+1916), leading to a factor $\sqrt{\frac{t_{\text{core}}}{t_{\text{FR606}}}} = \sqrt{\frac{3}{8.3}}$ in the radiometer equation. Other factors such as the sky background and the influence of zenith angle on the sensitivity should be mostly the same for both campaigns. Our S_{lim} is thus $\frac{22}{4} \sqrt{\frac{3}{8.3}} = 3.3$ times deeper than the [Grießmeier et al. \(2021\)](#) upper limit for

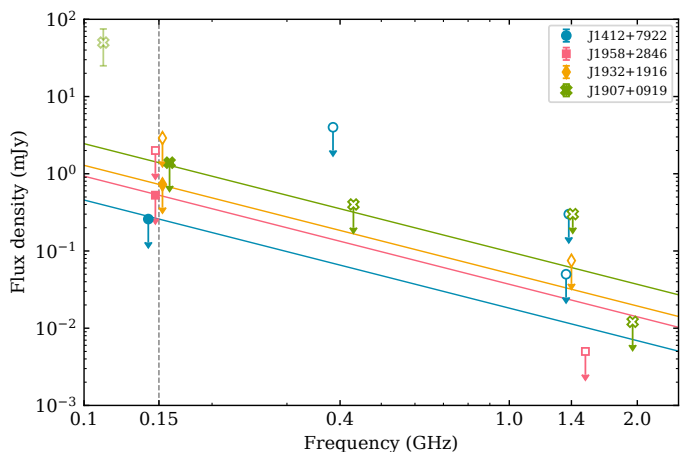


Fig. 1. Flux density upper limits of this work at 150 MHz (filled symbols) with $S/N = 5$ for comparison to earlier searches of the same sources (empty symbols). Solid lines going through our upper limit estimates with spectral index $\alpha = -1.4$ are overlaid to show the scaling of our sensitivity limits. Our limits are plotted slightly offset from the 150 MHz observing frequency (dashed line) for better visibility. The faded green marker for SGR J1907+0919 represents the claimed detection from Shitov et al. (2000).

J1958+2846, and 4.7 times for J1932+1916. Those factors are in good agreement with the actual limits listed in Table 1.

In Bilous et al. (2016), they measured the mean flux density S_{mean} of 158 pulsars detected with LOFAR, where $S_{\text{lim,p}} = S_{\text{mean}} \times \sqrt{W/(P-W)} = S_{\text{mean}}/3$. Compared to those LOFAR detections, our upper limit on J1412+7922 is deeper than all 158 sources (100%), J1958+2846 is deeper than 156 sources (99%), J1932+1916 is deeper than 144 sources (93%), and J1907+0919 is deeper than 109 sources (69%). The flux upper limits we have set on each of the sources in our sample are some of the deepest compared to other LOFAR radio pulsar detections. Longer observing times are thus unlikely to result in a detection or improve our flux upper limits. Additional follow up would only be constraining with more sensitive radio telescopes.

6.2. Emission angles and intensity

Different pulsar emission mechanism models exist that predict radio and γ -ray emission to be simultaneously formed in the pulsar magnetosphere. The emission sites are not necessarily collocated, though. The periodic radio emission is generally thought to be formed just above the polar cap. The high-energy polar cap (PC) model next assumes that the γ -ray emission is also produced near the surface of the NS, and near the magnetic polar caps. In the outer magnetosphere emission models, such as the Outer Gap (OG) or the One Pole Caustic (OPC) models, on the other hand, the γ -ray emission is produced high up in the magnetosphere of the NS, within the extent of the light cylinder.

For the sources in our sample, specific high-energy geometry models have only been proposed for J1958+2846 (Pierbattista et al. 2015). A detection could have confirmed one of these (Sect. 2.2). But also for our sample in general, conclusions can be drawn from the non-detections. The two general high-energy model classes mentioned above predict different, testable beam widths. Our radio non-detections, when attributed to radio beams that are not wide enough to encompass Earth, favor outer magnetospheric models (see, e.g., Romani & Watters 2010). That is because in the OG/OPC models, the γ -ray beam (which is de-

tected for our sources) is much broader than the radio beam. The radio beam, being much narrower, is unlikely cut through our line of sight. Such a model class is thus more applicable than one where the radio and high-energy beam are of similar angular size, such as the PC model (or, to a lesser extent, the slot gap model; Muslimov & Harding 2003; Pierbattista et al. 2015). In that case, detections in both radio and high-energy would be more often expected. Our results thus favor OG and OPC models over PC models for high-energy emission.

Note that while it is instructive to discuss the coverage of the radio pulsar beam in binary terms – it either hits or misses Earth – this visibility is not that unambiguous in practice. The beam edge is not sharp. In a beam mapping experiment enabled by the geometric precession in PSR J1906+0745 (van Leeuwen et al. 2015), the flux at the edge of the beam is over 100× dimmer than the peak, but it is still present and detectable (Desvignes et al. 2019). Deeper searches thus continue to have value, even if non-detections at the same frequency already exist.

That said, the detection of PSR J1732–3131 only at 327 and potentially even 34 MHz (Maan & Aswathappa 2014) shows that emission beam widening (or, possibly equivalently, a steep spectral index) at low frequencies is a real effect, also for γ -ray pulsars.

6.3. Emission mechanism and evolution

Most models explain the radio quietness of an NS through a chance beam misalignment, as above. It could, of course, also be a more intrinsic property. There are at least two regions in the P - \dot{P} diagram where radio emission may be increasingly hard to generate.

The first parameter space of interest is for sources close to the radio death line (Chen & Ruderman 1993). XDINSs are preferably found there, which suggests these sources are approaching, in their evolution, a state in which radio emission generally ceases. From what we see in normal pulsars, the death line represents the transition into a state in which electron-positron pair formation over the polar cap completely ceases. Once the pulsar rotates too slowly to generate a large enough potential drop over the polar cap, required for this formation, the radio emission turns off (Ruderman & Sutherland 1975). The high-energy emission also requires pair formation, but these could occur farther out. We note that polar cap pair formation can continue at longer periods, if the NS surface magnetic field is not a pure dipole. With such a decreased curvature radius, the NS may keep on shining. Evidence for such higher-order fields is present in a number of pulsars, e.g., PSR J0815+0939 (Szary & van Leeuwen 2017) and PSR B1839–04 (Szary et al. 2020). This would also influence the interpretation of any polarization information, as the RVM generally assumes a dipole field.

None of the sources in our sample are close to this death line (See Fig. 2), but SGR J1907+0919 is beyond a different, purported boundary: the photon splitting line (Baring & Harding 2001). In pulsars in that second parameter space of interest, where magnetic fields are stronger than the quantum critical field, of 4.4×10^{13} G (Fig. 2), pair formation cannot compete with magnetic photon splitting. Such high-field sources could then be radio quiet but X-ray or γ -ray bright. We mark the critical field line for a dipole in Fig. 2, but note, as Baring & Harding (2001) do, that higher multipoles and general relativistic effects can subtly change the quiescence limit on a per-source basis. That said, given its spindown dipole magnetic field strength of 7×10^{14} G, our non-detection of SGR J1907+0919 supports the existence of this limit.

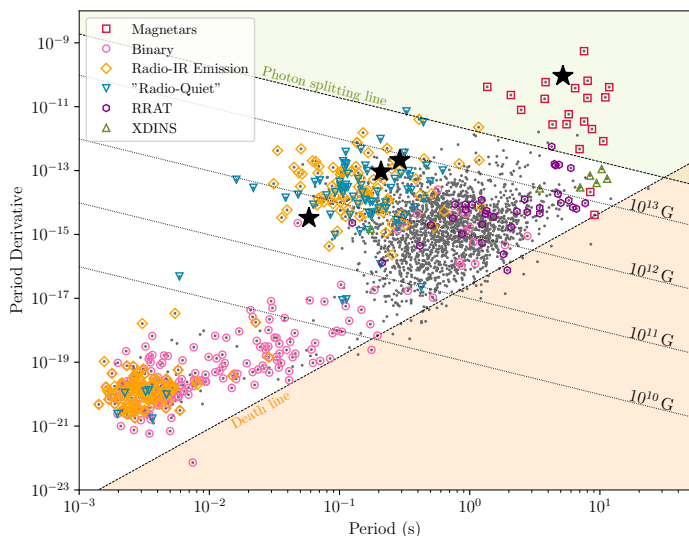


Fig. 2. $P - \dot{P}$ diagram showing the location of the sources presented in this work. All pulsars from the ATNF Pulsar Catalogue (Manchester et al. 2005) are shown as grey dots, with different pulsar classifications encircled by different symbols. The sources discussed in this work are shown as black stars, from left to right: J1412+7922, J1932+1916, J1932+1916, and J1907+0919. The orange shaded region is delimited by the death line, while the green shaded region is delimited by the photon splitting line. Plot generated with psrqpy (Pitkin 2018).

6.4. Propagation effects

While the emission beam widening and the negative spectral index provide potential advantages when searching for pulsars at low frequencies, some propagation effects such as dispersion and scattering intensify there, impeding detection of certain sources. The largest pulsar DM detected with LOFAR is 217 pc cm^{-3} , while many galactic pulsars are known to have $\text{DM} > 1000 \text{ pc cm}^{-3}$. Although the sources studied in this work do not have radio detections and thus no known DM, we can estimate this DM if a hydrogen column density N_{H} was measured from soft X-ray detections. He et al. (2013) find a correlation between N_{H} and DM as follows: $N_{\text{H}} (10^{20} \text{ cm}^{-2}) = 0.30^{+0.13}_{-0.09} \text{ DM} (\text{pc cm}^{-3})$.

While J1958+2846 and J1932+1916 have only been detected in γ -rays, J1412+7922 and J1907+0919 have soft X-ray detections where N_{H} has been measured. For J1907+0919, Kouveliotou et al. (1999) measured a large N_{H} value of $3.4 - 5.5 \times 10^{22} \text{ cm}^{-2}$. The correlation suggests a DM of $1100 - 1800 \text{ pc cm}^{-3}$. At such a large DM the detection limit of LOFAR is severely impacted. Because J1907+0919 is a very slow rotator, the intra channel dispersion delay still only becomes or order 10% of the period, which means periodicity searches could in principle still detect it; but the flux density per bin is of course much decreased when the pulse is smeared out over 100s of time bins.

In contrast, Shevchuk et al. (2009) reported a measured $N_{\text{H}} = 3.1 \pm 0.9 \times 10^{20} \text{ cm}^{-2}$ for J1412+7922. We thus estimate its DM to be in the range $5 - 15 \text{ pc cm}^{-3}$. This low DM would have easily been detected with LOFAR.

7. Conclusion

We have conducted deep LOFAR searches of periodic and single-pulse radio emission from four isolated neutron stars. Although we validated the observational setup with the detection of the test pulsars, we did not detect any of the four targeted pulsars.

This can be explained with an intrinsic radio-quietness of these sources, as was previously proposed. It could also be caused by a chance misalignment between the radio beam and the line of sight.

With the new upper limits, we can rule out the hypothesis that INSs had not been previously detected at radio frequencies around 1 GHz, because of a steeper spectrum than that of regular radio pulsars. Since radio emission from magnetars has been detected after high energy outbursts (e.g. Maan et al. 2022b), additional radio observations of J1907+0919 if the source reactivates might be successful at detecting single pulse or periodic emission in the future.

Acknowledgements. This research was supported by the Netherlands Research School for Astronomy (‘NOVA5-NW3-10.3.5.14’), the European Research Council under the European Union’s Seventh Framework Programme (FP/2007-2013)/ERC Grant Agreement No. 617199 (‘ALERT’), and by Vici research programme ‘ARGO’ with project number 639.043.815, financed by the Dutch Research Council (NWO). We further acknowledge funding from National Aeronautics and Space Administration (NASA) grant number NNX17AL74G issued through the NNN16ZDA001N Astrophysics Data Analysis Program (ADAP) to SMS. This paper is based (in part) on data obtained with the International LOFAR Telescope (ILT) under project code LC3_036 (PI: van Leeuwen). LOFAR (van Haarlem et al. 2013) is the low frequency array designed and constructed by ASTRON. It has observing, data processing, and data storage facilities in several countries, that are owned by various parties (each with their own funding sources), and that are collectively operated by the ILT foundation under a joint scientific policy. The ILT resources have benefitted from the following recent major funding sources: CNRS-INSU, Observatoire de Paris and Université d’Orléans, France; BMBF, MIWF-NRW, MPG, Germany; Science Foundation Ireland (SFI), Department of Business, Enterprise and Innovation (DBEI), Ireland; NWO, The Netherlands; The Science and Technology Facilities Council, UK; Ministry of Science and Higher Education, Poland.

References

- Abdo, A. A., Ackermann, M., Ajello, M., et al. 2009, *Science*, **325**, 840
 Abdo, A. A., Ajello, M., Allafort, A., et al. 2013, *ApJS*, **208**, 17
 Alexov, A., Hessels, J., Mol, J. D., Stappers, B., & van Leeuwen, J. 2010, *Astronomical Data Analysis Software and Systems XIX*, 434
 Arias, M., Botteon, A., Bassa, C. G., et al. 2022, *Astronomy & Astrophysics*, **667**, A71
 Baring, M. G. & Harding, A. K. 2001, *ApJ*, **547**, 929
 Bates, S. D., Lorimer, D. R., & Verbiest, J. P. W. 2013, *Monthly Notices of the Royal Astronomical Society*, **431**, 1352
 Bilous, A., Kondratiev, V., Kramer, M., et al. 2016, *Astronomy & Astrophysics*, **591**, A134
 Bochenek, C. D., Ravi, V., Belov, K. V., et al. 2020, *Nature*, **587**, 59
 Bogdanov, S., Ho, W. C. G., Enoto, T., et al. 2019, *arXiv:1902.00144 [astro-ph]*, arXiv: 1902.00144
 Burke-Spolaor, S. 2012, *Proceedings of the International Astronomical Union*, **8**, 95
 Caleb, M., Heywood, I., Rajwade, K., et al. 2022, *Nature Astronomy*, **1**
 Camilo, F., Ransom, S. M., Halpern, J. P., et al. 2006, *Nature*, **442**, 892
 Chen, J. L. & Wang, H. G. 2014, *The Astrophysical Journal Supplement Series*, **215**, 11
 Chen, K. & Ruderman, M. 1993, *ApJ*, **402**, 264
 Cheng, K. S., Ruderman, M., & Zhang, L. 2000, *The Astrophysical Journal*, **537**, 964
 CHIME/FRB Collaboration. 2020, *Nature*, **587**, 54
 Clark, C. J., Wu, J., Pletsch, H. J., et al. 2017, *The Astrophysical Journal*, **834**, 106, arXiv: 1611.01015
 Coenen, T. 2013, PhD thesis, University of Amsterdam, <http://dare.uva.nl/en/record/459730>
 Coenen, T., van Leeuwen, J., Hessels, J. W. T., et al. 2014, *Astronomy & Astrophysics*, **570**, A60
 Connor, L. & van Leeuwen, J. 2018, *The Astronomical Journal*, **156**, 256
 Connor, L., van Leeuwen, J., Oostrum, L. C., et al. 2020, *Monthly Notices of the Royal Astronomical Society*, **499**, 4716
 Cordes, J. M. 1978, *The Astrophysical Journal*, **222**, 1006
 Desvignes, G., Kramer, M., Lee, K., et al. 2019, *Science*, **365**, 1013
 Dewey, R. J., Taylor, J. H., Weisberg, J. M., & Stokes, G. H. 1985, *ApJ*, **294**, L25
 Fox, D. W., Kaplan, D. L., Kulkarni, S. R., & Frail, D. A. 2001, *arXiv:astro-ph/0107520*

- Frail, D. A., Jagannathan, P., Mooley, K. P., & Intema, H. T. 2016, *The Astrophysical Journal*, 829, 119
- Frail, D. A., Kulkarni, S. R., & Bloom, J. S. 1999, *Nature*, 398, 127
- Gençali, A. A. & Ertan, Ü. 2018, *Monthly Notices of the Royal Astronomical Society*, 481, 244
- Grieffmeier, J. M., Smith, D. A., Theureau, G., et al. 2021, *A&A*, 654, A43
- Haberl, F. 2007, *Ap&SS*, 308, 181
- Halpern, J. P., Bogdanov, S., & Gotthelf, E. V. 2013, *The Astrophysical Journal*, 778, 120
- He, C., Ng, C.-Y., & Kaspi, V. M. 2013, *The Astrophysical Journal*, 768, 64
- Hessels, J. W. T., Stappers, B. W., Rutledge, R. E., Fox, D. B., & Shevchuk, A. H. 2007, *Astronomy & Astrophysics*, 476, 331
- Hewish, A., Bell, S. J., Pilkington, J. D. H., Scott, P. F., & Collins, R. A. 1968, *Nature*, 217, 709
- Hotan, A. W., van Straten, W., & Manchester, R. N. 2004, *Publications of the Astronomical Society of Australia*, 21, 302
- Hurley, K., Li, P., Kouveliotou, C., et al. 1999, *The Astrophysical Journal*, 510, 111
- Hurley-Walker, N., Zhang, X., Bahramian, A., et al. 2022, *Nature*, 601, 526
- Jankowski, F., van Straten, W., Keane, E. F., et al. 2018, *Monthly Notices of the Royal Astronomical Society*, 473, 4436
- Karpova, A., Shternin, P., Zyuzin, D., Danilenko, A., & Shibanov, Y. 2017, *Monthly Notices of the Royal Astronomical Society*, 466, 1757
- Keane, E. F., Kramer, M., Lyne, A. G., Stappers, B. W., & McLaughlin, M. A. 2011, *MNRAS*, 415, 3065
- Komesaroff, M. M. 1970, *Nature*, 225, 612
- Kondratiev, V. I., McLaughlin, M. A., Lorimer, D. R., et al. 2009, *The Astrophysical Journal*, 702, 692
- Kondratiev, V. I., Verbiest, J. P. W., Hessels, J. W. T., et al. 2016, *Astronomy & Astrophysics*, 585, A128
- Kouveliotou, C., Fishman, G. J., Meegan, C. A., et al. 1993, *Nature*, 362, 728
- Kouveliotou, C., Strohmayer, T., Hurley, K., et al. 1999, *The Astrophysical Journal*, 510, 115
- Lazarus, P., Kaspi, V. M., Champion, D. J., Hessels, J. W. T., & Dib, R. 2012, *The Astrophysical Journal*, 744, 97
- Lorimer, D. R. & Xilouris, K. M. 2000, *The Astrophysical Journal*, 545, 385
- Maan, Y. 2015, *ApJ*, 815, 126
- Maan, Y. & Aswathappa, H. A. 2014, *Monthly Notices of the Royal Astronomical Society*, 445, 3221
- Maan, Y., Surnis, M. P., Chandra Joshi, B., & Bagchi, M. 2022a, *ApJ*, 931, 67
- Maan, Y., van Leeuwen, J., Straal, S., & Pastor-Marazuela, I. 2022b, *The Astronomer's Telegram*, 15697, 1
- Malofeev, V. M. & Malov, O. I. 1997, *Nature*, 389, 697
- Malov, O. I., Malofeev, V. M., Teplykh, D. A., & Logvinenko, S. V. 2015, *Astronomy Reports*, 59, 183
- Manchester, R. N., Hobbs, G. B., Teoh, A., & Hobbs, M. 2005, *The Astronomical Journal*, 129, 1993
- Mazets, E. P., Golenetskii, S. V., & Guryan, Y. A. 1979, *Soviet Astronomy Letters*, 5, 343
- Mereghetti, S., Rigoselli, M., Taverna, R., et al. 2021, *ApJ*, 922, 253
- Mereghetti, S., Esposito, P., Tiengo, A., et al. 2006, *The Astrophysical Journal*, 653, 1423
- Mikhailov, K. & van Leeuwen, J. 2016, *Astronomy & Astrophysics*, 593, A21
- Morello, V., Keane, E. F., Enoto, T., et al. 2020, *MNRAS*, 493, 1165
- Muslimov, A. G. & Harding, A. K. 2003, *ApJ*, 588, 430
- Oostrum, L. C., van Leeuwen, J., Maan, Y., Coenen, T., & Ishwara-Chandra, C. H. 2020, *MNRAS*, 492, 4825
- Pastor-Marazuela, I. 2022, PhD Thesis, University of Amsterdam
- Pastor-Marazuela, I., Connor, L., van Leeuwen, J., et al. 2021, *Nature*, 596, 505
- Pastor-Marazuela, I., van Leeuwen, J., Bilous, A., et al. 2022, *arXiv:2202.08002 [astro-ph]*
- Pierbattista, M., Harding, A. K., Grenier, I. A., et al. 2015, *Astronomy & Astrophysics*, 575, A3
- Pires, A. M., Haberl, F., Zavlin, V. E., et al. 2014, *Astronomy & Astrophysics*, 563, A50, *arXiv: 1401.7147*
- Pitkin, M. 2018, *The Journal of Open Source Software*, 3, 538
- Pletsch, H. J., Guillemot, L., Allen, B., et al. 2013, *The Astrophysical Journal*, 779, L11, *arXiv: 1311.6427*
- Radhakrishnan, V. & Cooke, D. J. 1969, *Astrophysical Letters*, 3, 225
- Ransom, S. M. 2001, PhD thesis, Harvard University
- Ray, P. S., Kerr, M., Parent, D., et al. 2011, *The Astrophysical Journal Supplement Series*, 194, 17
- Rigoselli, M., Mereghetti, S., Suleimanov, V., et al. 2019, *A&A*, 627, A69
- Romani, R. W. & Watters, K. P. 2010, *The Astrophysical Journal*, 714, 810
- Rookyard, S. C., Weltevrede, P., & Johnston, S. 2015, *MNRAS*, 446, 3367
- Ruderman, M. A. & Sutherland, P. G. 1975, *ApJ*, 196, 51
- Rutledge, R. E., Fox, D. B., & Shevchuk, A. H. 2008, *The Astrophysical Journal*, 672, 1137
- Sanidas, S., Cooper, S., Bassa, C. G., et al. 2019, *Astronomy & Astrophysics*, 626, A104
- Shevchuk, A. S. H., Fox, D. B., & Rutledge, R. E. 2009, *The Astrophysical Journal*, 705, 391
- Shitov, Y. P., Pugachev, V. D., & Kutuzov, S. M. 2000, *Pulsar Astronomy - 2000 and Beyond*, 202
- Stappers, B. W., Hessels, J. W. T., Alexov, A., et al. 2011, *Astronomy & Astrophysics*, 530, A80
- Szary, A. & van Leeuwen, J. 2017, *ApJ*, 845, 95
- Szary, A., van Leeuwen, J., Weltevrede, P., & Maan, Y. 2020, *The Astrophysical Journal*, 896, 168
- Tan, C. M., Bassa, C. G., Cooper, S., et al. 2018, *ApJ*, 866, 54
- van Haarlem, M. P., Wise, M. W., Gunst, A. W., et al. 2013, *Astronomy & Astrophysics*, 556, A2
- van Leeuwen, J. 2014, in *The Third Hot-wiring the Transient Universe Workshop (HTU-III)*, Santa Fe, NM, 79
- van Leeuwen, J. & Stappers, B. W. 2010, *A&A*, 509, 7
- van Leeuwen, J., Kasian, L., Stairs, I. H., et al. 2015, *ApJ*, 798, 118
- van Leeuwen, J., Kooistra, E., Oostrum, L., et al. 2022, *arXiv:2205.12362 [astro-ph]*
- Voges, W., Aschenbach, B., Boller, T., et al. 1999, *Astronomy and Astrophysics*, 349, 389
- Watters, K. P., Romani, R. W., Weltevrede, P., & Johnston, S. 2009, *The Astrophysical Journal*, 695, 1289
- Young, M. D., Manchester, R. N., & Johnston, S. 1999, *Nature*, 400, 848
- Zane, S., Haberl, F., Israel, G. L., et al. 2011, *Monthly Notices of the Royal Astronomical Society*, 410, 2428